PRELIMINARY CONSIDERATIONS FOR NEAR'S LOW-ALTITUDE PASSES AND LANDING OPERATIONS AT 433 EROS[1]

P. G. Antreasian[†], C. L. Helfrich[†], J. K. Miller[†], W. M. Owen[†],
B. G. Williams[‡], D. K. Yeomans[‡], J. D. Giorgini[‡]
Jet Propulsion Laboratory, California Institute of Technology,
Pasadena, CA 91109-8099
and
D. W. Dunham[2], R. W. Farquhar[2], J. V. McAdams[2]
The Johns Hopkins University, Applied Physics Laboratory,
Johns Hopkins Road, Laurel, MD 20723
and
D.J. Scheeres[†]
Dept. of Aerospace Engineering and Engineering Mechanics, Iowa State University,
Ames, IA 50011

Abstract

NASA's Near Earth Asteroid Rendezvous (NEAR) mission is currently on course for rendezvous and orbit insertion about the asteroid 433 Eros in December 1998. The plan is to establish an orbit of the NEAR spacecraft with increasingly lower altitudes as the one year orbit phase progresses. This paper is concerned with options for mission design and navigation during for the last two months of the orbit phase, where several close passes to the surface could be incorporated to enhance the science return. Two feasible low altitude designs exist: 1) tight retrograde orbits, and 2) low passes with perigee located at specific regions relative to the surface of Eros. These close passes will culminate with a landing on the surface which will mark the end the NEAR mission. This paper will investigate the navigational accuracies associated with these close passes and landing scenarios.

INTRODUCTION

NASA's Discovery-class Near Earth Asteroid Rendezvous (NEAR) mission is *nearing* its final goal of rendezvous and orbit about the S-type asteroid 433 Eros starting in December 1998. Since the time of its discovery approximately 100 years ago, an extensive set of ground-based observations have determined 433 Eros to be an irregularly shaped body measuring 20 km by 40 km overall, with a rotational period of 5.27 hours and its rotational pole nearly aligned in the plane of its orbit[1]. The primary objectives of the NEAR mission are to obtain unprecedented close-up physical and geological observations of a near-Earth asteroid. The NEAR mission is being operated by the Applied Physics Laboratory of Johns Hopkins University, while navigation of the spacecraft is being provided by the Jet Propulsion Laboratory, California Institute of Technology. Launched in February of 1996, the NEAR spacecraft (S/C) flew by the C-class asteroid Mathilde in late June of 1997 enroute to Eros. One week later, a Deep Space Maneuver was performed to place S/C on a trajectory for a gravity assist at Earth. On January 23rd of 1998, NEAR flew by Earth in such a way as to gain the necessary energy in which to alter its heliocentric inclination, thereby placing it on course for rendezvous with Eros ($i \approx 10.8°$). For a general description of the NEAR mission and the design of its interplanetary trajectory, see Farquhar et al.[2].

The NEAR S/C will perform a series of rendezvous maneuvers in December of 1998 to slow its speed with respect to Eros. On January 10th of 1999, an orbit insertion burn will execute to place the S/C into orbit around Eros. NEAR will initially orbit Eros with distances ranging from 1000 to 200 km in order to characterize the shape, gravity and spin of Eros. Once the physical parameters of Eros are determined reasonably well, the plan is to establish an orbit of the NEAR S/C with increasingly lower altitudes as the one year orbit phase progresses while further characterizing the gravity and shape of Eros. The navigation during this phase relies

[1] AIAA Paper 98-4397.

[2] Member Technical Staff, Navigation and Flight Mechanics Section

[3] Member Technical Staff, Navigation and Flight Mechanics Section, Member AIAA

[4] Senior Member AIAA, Member AAS

on a combination of NASA's Deep Space Network (DSN) radio metric tracking, laser ranging (LIDAR) data from the S/C to the surface of Eros, and on board optical imaging of landmarks on Eros. For a description of the NEAR navigation systems used for orbit and attitude control, see Miller et al.[3]. Miller et al.[3] also describes the expected navigational accuracies for orbit prediction and control as well as the expected accuracies of the key parameters that model the physical properties of Eros described above during the rendezvous and orbital phases of the mission. The expected orbital characteristics of NEAR due to the complex dynamical environment at Eros and methods for orbit control during the orbit phase are discussed by Scheeres[4]. The various aspects of trajectory design for the orbital phase are detailed by Miller et al.[5].

Towards the end of the NEAR mission after the shape, gravity and spin of Eros have been well characterized, the scientific interest of obtaining very close observations (< 5 km) can be realized provided the mission is willing to allow for additional risk. Discussed in this paper are several options for mission design and navigation during the last two months of the orbit phase, where several close passes to within a couple of kilometers of the surface could be incorporated to enhance the science return. At close altitudes, the strong perturbations from the irregular gravity field of Eros cause large changes to orbit energy and eccentricity. These effects can lead to unstable situations where either the spacecraft is suddenly placed on an escape or impact trajectory. By defining an averaged potential for the ellipticity effect from the gravity harmonic, C_{22}, on the S/C's orbit, the basic form of equations for the changes in energy, and angular momentum during an orbit are derived. With the consideration of the variation of these parameters for orbit design, two feasible approaches have been analyzed to effect low altitude flybys of the Eros surface, enabling high-resolution imagery and localized gravitational measurements. This paper will discuss plans and expected navigational accuracies for two types of low altitude passes: (1) tight retrograde orbits which have the drawback of high relative velocity with the surface, and (2) targeted low passes to some latitude and longitude which have the possibility of smaller relative velocity with the surface.

These close passes will culminate with a landing on the surface of Eros which will mark the end of the NEAR mission. A conservative approach is given for the landing phase while allowing for very close observations (~ 1.2 km). The design considers placing the S/C into a polar orbit about Eros and performing a deorbit maneuver at the pole. At a pre-determined time before impact, a slow down maneuver is performed, then once the S/C reaches a desired altitude, an escape maneuver is performed to place the S/C back into orbit about Eros. This sequence can be repeated by being less conservative until eventual impact. The navigational challenge in this scenario is to minimize the impact speed such that the S/C remains on the surface of Eros. The navigational accuracies associated with this design are presented. If a low impact speed is desired, altimetry data acquired from the LIDAR instrument (as well as landmark tracking) could allow for autonomous landing. Three designs ranging from simple to complex are discussed for implementing an autonomous on board navigation filter.

MISSION CONSTRAINTS

Orbit Constraints

Because of the fixed mounting of the science instruments, solar array and high gain antenna, the NEAR mission must operate under several constraints during the orbit phase to ensure the health and safety of the spacecraft while providing near continuous coverage for valuable science[3]. To ensure adequate illumination of the solar arrays for power, the S/C's attitude must be such that the normal of the solar arrays remains within 30° of the Sun direction vector. Because of this and the additional constraint that the science instruments must always point nadir, the orbit plane must be oriented such that the orbit normal remain within 30 degrees of the Sun. Tracking also imposes a constraint that the orbit normal remain within 30 degrees of the Earth direction to ensure navigation data and science return. By controlling the S/C's orbit inclination, radius and argument of ascending node, these mission constraints can be met[4]. In addition, so that the S/C never loses power, the S/C is constrained to never fly into the shadow of Eros.

Orbit Stability

Orbit stability should also be considered as imposing constraints on mission design for low altitude passes. These constraints include:

- No direct orbits ($i < 90°$) within 50 km of Eros
- No polar orbits within 50 km of Eros unless specifically verified first (depending on the precise Eros parameters there may be destabilizing resonances from 50 km on down).
- All nominal close orbits will be retrograde, initially within 10° of the equator perhaps higher following additional Eros parameter characterization.

Tracking Requirements

During critical periods of the orbit phase, such as initial orbit characterization for lower altitude orbits, continuous X-Band Doppler coverage will be required from the DSN's 34 m and 70 m antennas. During the entire orbit phase, landmark tracking images will be acquired at the rate of 8 images per day. Continuous Doppler coverage of propulsive maneuver events will be required from 2 days prior to 1 day after. In addition, two landmark images taken immediately before and two after maneuver execution will be required. Currently, there's no navigational requirement for LIDAR coverage. Because of the criticality of the low pass orbits, and landing scenarios that will be described below, it is assumed for this study that continuous Doppler tracking will be provided.

Maneuver Design

Orbit correction maneuvers (OCMs) will be required from time to time to maintain the orbit constraints or to target the trajectory for science purposes. A number of steps in ground operations are performed before an OCM executes, such as maneuver design, implementation, sequence generation, verification and uplink. Because of time required to perform these steps, it is necessary to allow approximately one week for preparation before OCM execution. If a maneuver fails to execute, and/or the S/C's orbit becomes unstable such that it may eventually impact or escape, it will be necessary to execute a maneuver as quickly as possible. Under such circumstances, the minimum time required to redetermine the S/C's orbit, and uplink a new maneuver sequence is set at approximately three hours.

LOW-ALTITUDE PASS DESIGN & NAVIGATION

Designing and navigating a close, tight orbit about a body as distended as Eros presents unique challenges, and is an unprecedented orbital situation. The dynamics of S/C close to such a body are subject to strong perturbations from the gravity field, the major contribution coming from the 2nd degree and order gravity field, which can be reduced to the two terms C_{20} (oblateness) and C_{22} (ellipticity). Each of these terms has a unique contribution to the evolution of the S/C orbit, the oblateness causing secular increase in the orbit plane (node), periapsis argument, and mean anomaly; the ellipticity causing changes in the orbit semi-major axis, eccentricity and inclination. Thus these two gravity terms cause substantive changes in all six orbital elements. For Eros planning purposes, the assumed values of these two gravity coefficients are:

$$r_o^2 C_{20} = -12.267 \text{ km}^2 \quad (1)$$

$$r_o^2 C_{22} = 15.718 \text{ km}^2 \quad (2)$$

The actual value of these terms, of course, will not be determined until after Eros rendezvous. The assumed value of the gravitational parameter is:

$$\mu = 6.546 \times 10^{-4} \quad (3)$$

The effect of the oblateness is troublesome as it causes the orbit plane to precess, but in and of itself does not cause instability in the orbit. The effect of the ellipticity, however, can cause severe instabilities in the S/C orbit as it directly modifies the energy and angular momentum during each orbit. The reason for this effect is due to resonances between the orbit period and the asteroid rotation rate (which has a period of 5.27 hours for Eros). The changes in orbit energy can be severe enough to cause an initially bound orbit (negative energy) to become hyperbolic (positive energy) following a single periapsis passage or, conversely, capture a hyperbolic orbit into an elliptic orbit following periapsis passage. More importantly, from a stability point of view, this perturbation can cause the orbit periapsis to decrease, setting up the potential for an impact with the asteroid surface. Fortunately, this effect and the size of the perturbations experienced per orbit can be accurately quantified analytically and designed to minimize S/C risk. A more detailed discussion of these perturbations for small-body orbiters is given in [6]. The essential results of that discussion are given below.

Since the effect of asteroid ellipticity can cause such large changes to orbit energy and eccentricity, it is preferable, from an analytic point of view, to characterize these perturbations in terms of the orbit energy, $C_2 = -\mu/(2a)$, angular momentum, $h = \sqrt{\mu a(1-e^2)}$, and projection of angular momentum onto the asteroid pole axis, $H = h\cos i$. Defining an "averaged" potential for the C_{22} term, $\tilde{R}_{22}$, and evaluating changes in these three parameters yields secular differential equations:

$$\begin{aligned}\tilde{R}_{22} = {} & \frac{3\mu C_{22}}{2\pi q^3}\sqrt{\frac{(1-e)^3}{(1+e)}} \\ & \Big[\frac{1}{2}\sin^2 i\left(\cos 2\Omega I_0^1 - \sin 2\Omega J_0^1\right) \\ & + \cos^4(i/2)\left(\cos 2(\omega+\Omega) I_2^1 \right. \\ & \left. - \sin 2(\omega+\Omega) J_2^1\right) \\ & + \sin^4(i/2)\left(\cos 2(\omega-\Omega) I_{-2}^1 \right. \\ & \left. + \sin 2(\omega-\Omega) J_{-2}^1\right)\Big] \end{aligned} \quad (4)$$

$$\dot{C}_2 = n\frac{\partial \tilde{R}_{22}}{\partial M} \quad (5)$$

$$\dot{h} = \frac{\partial \tilde{R}_{22}}{\partial \omega} \quad (6)$$

$$\dot{H} = \frac{\partial \tilde{R}_{22}}{\partial \Omega} \quad (7)$$

where a is the semi-major axis, e is the eccentricity, i is the inclination measured from the Eros rotation pole, Ω is the ascending node measured in the body-fixed frame, ω is the argument of periapsis measured in the body-fixed frame and M is the mean anomaly. The functions I_m^n and J_m^n are defined as the integrals:

$$\begin{aligned} I_m^n(e,k) = {} & \int_{-\theta_\infty}^{\theta_\infty}\left(\frac{1+e\cos f}{1+e}\right)^n \\ & \cos(mf - 2kM)df \end{aligned} \quad (8)$$

$$\begin{aligned} J_m^n(e,k) = {} & \int_{-\theta_\infty}^{\theta_\infty}\left(\frac{1+e\cos f}{1+e}\right)^n \\ & \sin(mf - 2kM)df \end{aligned} \quad (9)$$

where $\theta_\infty = \pi$ if $e \le 1$, and $\theta_\infty = \cos^{-1}(-1/e)$ if $e > 1$, f is the true anomaly of the orbit (defined for elliptic, parabolic and hyperbolic orbits), M is the generalized mean anomaly of the orbit (which is a function of true anomaly for either an elliptic, parabolic or hyperbolic orbit) and $k = 2\pi/(Tn)$, where T is the rotation period of the asteroid and n is the mean motion of the spacecraft orbit (or its generalization for hyperbolic orbits) and can also be expressed as:

$$k = \sqrt{\frac{3\pi}{G}\frac{\tilde{a}^3}{\rho T^2}} \quad (10)$$

where G is the gravitational constant (6.672×10^{-8} cm^3/g/s^2), $\tilde{a}$ is the normalized semi-major axis and ρ is the density in g/cm^3.

A subtle point must be made regarding the partial of $\tilde{R}_{22}$ with respect to the mean anomaly M. This differentiation must occur within the I_m^n and J_m^n integrals and only involves the true anomaly terms, f, present in the original, un-averaged potential. After this differentiation the I_m^n integrals can be expressed as a combination of the J_m^n integrals and are all zero while the J_m^n integrals can be expressed in terms of the I_m^n integrals. The specific computation of interest is the change in these variables over one orbit. To compute this, multiply each of the equations by $2\pi/n$ to yield:

$$\begin{aligned}\Delta C_2 &= -6r_o^2 C_{22}\frac{\mu}{q^3} \\ &\quad \left[\cos^4 i/2 \sin 2(\omega+\Omega)\right. \\ &\quad \left\{I_2^3 + \frac{3e}{4(1+e)}(I_3^2 - I_1^2)\right\} \\ &\quad + \sin^4 i/2 \sin 2(\omega-\Omega) \\ &\quad \left\{I_{-2}^3 + \frac{3e}{4(1+e)}(I_{-3}^2 - I_{-1}^2)\right\} \\ &\quad + \frac{3e}{8(1+e)}\sin^2 i \sin 2(\Omega) \\ &\quad \left.\{I_1^2 - I_{-1}^2\}\right] \qquad (11)\end{aligned}$$

$$\begin{aligned}\Delta h &= -6r_o^2 C_{22}\sqrt{\frac{\mu}{q^3(1+e)}} \\ &\quad \left[\cos^4 i/2 \sin 2(\omega+\Omega) I_2^1\right. \\ &\quad \left. + \sin^4 i/2 \sin 2(\omega-\Omega) I_{-2}^1\right] \qquad (12)\end{aligned}$$

$$\begin{aligned}\Delta H &= -6r_o^2 C_{22}\sqrt{\frac{\mu}{q^3(1+e)}} \\ &\quad \left[\cos^4 i/2 \sin 2(\omega+\Omega) I_2^1\right. \\ &\quad - \sin^4 i/2 \sin 2(\omega-\Omega) I_{-2}^1 \\ &\quad \left. + \frac{1}{2}\sin^2 i \sin 2\Omega I_0^1\right] \qquad (13)\end{aligned}$$

A careful derivation of all these equations show that they are valid for both elliptic ($e < 1$), parabolic ($e = 1$) and hyperbolic ($e > 1$) orbits. Also useful for describing the effect of the asteroid's ellipticity on the orbit are the linearized expressions for the change in orbit periapsis, eccentricity and inclination over one orbit:

$$\Delta q = \frac{q}{2e}\left[2(1+e)\frac{\Delta h}{h} + (1-e)\frac{\Delta C_2}{C_2}\right] \qquad (14)$$

$$\Delta e = \frac{-(1-e^2)}{2e}\left[2\frac{\Delta h}{h} + \frac{\Delta C_2}{C_2}\right] \qquad (15)$$

$$\Delta i = \cot i\frac{\Delta h}{h} - \csc i\frac{\Delta H}{h} \qquad (16)$$

The change in orbit size and shape can be completely normalized in terms of the body's size. Thus, the change in shape and size is only a function of the orbit shape (eccentricity) and relative size (periapsis radius expressed in terms of body radii). The body dependent terms which enter the expressions are the non-dimensional gravity coefficient C_{22} and k, where $k \propto 1/\sqrt{\rho T^2}$. Thus the body density and rotation period are combined into one parameter $\gamma = \sqrt{\rho T^2}$. This allows for general statements to be made about the dynamics of small body orbiters with a reduced set of asteroid parameters.

For the purposes of the current discussion it is sufficient to note the basic form of the perturbations to these parameters:

$$\begin{aligned}\Delta C_2 &\propto -6r_o^2 C_{22}\frac{\mu}{q^3} \\ &\quad \cos^4 i/2 \sin 2(\omega+\Omega) \qquad (17)\end{aligned}$$

$$\begin{aligned}\Delta h &\propto -6r_o^2 C_{22}\sqrt{\frac{\mu}{q^3(1+e)}} \\ &\quad \cos^4 i/2 \sin 2(\omega+\Omega) \qquad (18)\end{aligned}$$

$$\begin{aligned}\Delta H &\propto -6r_o^2 C_{22}\sqrt{\frac{\mu}{q^3(1+e)}} \\ &\quad \cos^4 i/2 \sin 2(\omega+\Omega) \qquad (19)\end{aligned}$$

since the integrals I_m^{-n} in Equations 11 - 13 generally have a small contribution to the perturbations, as the arguments of the cosine term in the integrand add and hence average to a smaller value. Thus we see that the dominant terms scale with $\cos^4(i/2)$, leading to a minimal contribution when the orbit is near retrograde ($i \sim \pi$) and to the largest effect when the orbit is direct ($i \sim 0$). Also the geometry of the orbit periapsis relative to the asteroid is also important in determining the effect. Basically, if $\tilde{\omega} = \Omega + \omega$ equals 0, $\pi/2$, π or $3\pi/2$ the net effect of the perturbations are zero. If $\tilde{\omega}$ lies in the first or third quadrant (i.e., lies over the leading edge of the rotating asteroid) the net change in energy is negative, leading to a decrease in semi-major axis. Conversely, if $\tilde{\omega}$ lies in the second or fourth quadrant (i.e., lies over the trailing edge of the rotating asteroid) the net change in energy is positive and the semi-major axis (and orbit period) increases. These results can be used to design simple and safe approaches to flying close to the asteroid.

Tight Retrograde Orbits

The first approach is to utilize the relatively small perturbations that retrograde orbits experience to fly close to the asteroid in a retrograde orbit in the equatorial plane. The analysis of stability of these orbits, indicated by the above analytical discussion, can be probed more deeply by computing periodic orbits about the asteroid and evaluating their stability. This has been done, using the model Eros shape, following procedures discussed in previous publications ([9], [4], [8]). Note that no approximations have been introduced in the computation of these orbits, and that a full gravity field (of 16th degree and order) has been used in their computation. Figure 1 shows the orbit radius vs. body-relative speed of this class of retrograde orbits. Note that this family is stable except for two intervals close to the asteroid. The first, near 22 kilometers, corresponds to a simple out-of-plane

hyperbolic instability and is probably due to a resonance between the asteroid rotation and the secular precession of the orbit plane. The second, near 19 kilometers, is complex-unstable and thus operates both out of the orbital plane and in the orbital plane, and is probably due to a resonance between the asteroid and the secular advance in the argument of periapsis. The second instability is more troublesome as it may lead to changes in the semi-major axis and eccentricity. A conservative limit on a retrograde orbit radius would be above 22 kilometers, to ensure that neither of these unstable intervals are encountered.

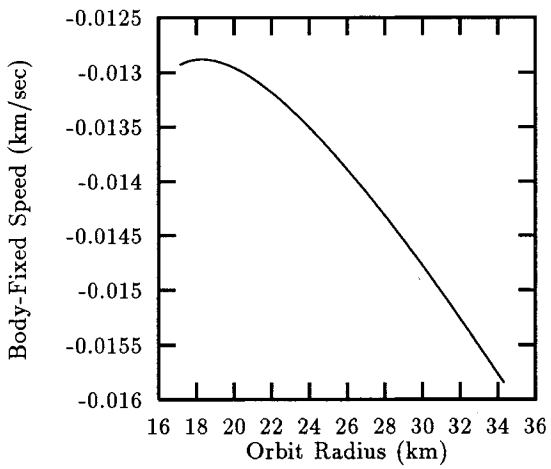

Figure 1: Retrograde family of orbits about Eros.

Tight Retrograde Orbit Navigation

Several retrograde orbits have been examined for close flybys of the ends of the asteroids. One circular 25 km orbit with inclination = 170° has been found to be stable for the current set of assumptions regarding the physical parameters of Eros. Orbits with lower radii were found to have extremely large variations in eccentricity which would be unacceptable for navigation. Figure 2 shows the 25 km orbit in the Eros-Mean-Equator inertial frame. The APL shape model of Eros as described by Miller et al.[3] is shown for comparison. Note that the asteroid rotates in the right-hand sense about the Eros-fixed z-axis which describes the instantaneous rotational pole in this frame, while the S/C moves around the asteroid in the opposite (retrograde) direction.

A detailed covariance analysis of this tight retrograde orbit (radius of 25 km, $i = 170°$) has been performed. This analysis takes a similar approach to the navigational strategies and orbit determination techniques as those presented by Miller et al.[3]. In this analysis, it is assumed that the physical parameters of Eros such as gravity shape and spin state will be well known. The gravity harmonics through degree and order eight will be well characterized by the time NEAR enters the 35 km orbit[3].

A 10 day data arc consisting of continuous 2-way coherent X-Band Doppler and up to 8 landmark images per day was simulated. The Doppler data was compressed to one average point per 600 seconds and was weighted at 0.012 Hz (0.2 mm/s) for an average count time of 60 seconds. The optical landmark images were weighted at 1 pixel in both line (vertical) and pixel (horizontal) directions. A maneuver was inserted at one day prior to the end of the data arc. In addition to the spacecraft's epoch state, the parameters that are estimated include maneuver ΔV, the asteroid physical parameters such as gravity harmonics to degree and order 7, the pole direction, the spin state, landmark positions, solar radiation pressure, and stochastic accelerations. To add conservatism, 8th degree and order gravity harmonic uncertainties of 100% were considered as well as DSN station location errors. The a priori uncertainties applied in the filter include a epoch state of 10 Mkm, 10 km/s, a 10% solar radiation pressure error, a spherical maneuver error of 5 mm/s, gravity harmonics at 100% error, landmarks locations at 4 m, the three Euler angles that describe the location of the pole and meridian of Eros with respect to Earth-Mean-Equator of 2000 (EME2000) at 20°, the 3-axis body-fixed spin rates at 0.02° per second, inertia tensor at 0.001 km^2 for each moment and product of inertia component.

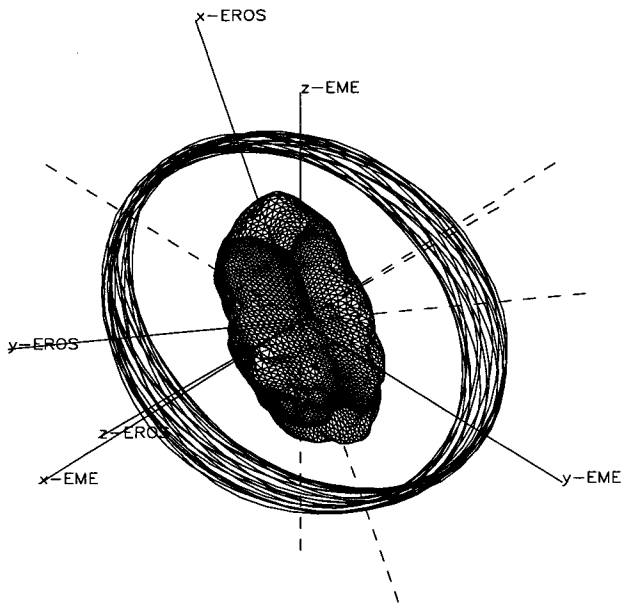

Figure 2: Oblique view of the 25 km orbit in the Eros-Mean-Equator inertial frame.

To maintain the orbital constraints or to target to the trajectory for science purposes during these tight orbits, OCM's will occasionally be required. As mentioned beforehand, under normal operations a period of 7 days is allowed for maneuver design. Therefore, the OCM is designed from an orbit solution with a tracking Data Cut-off (DCO) approximately one week before maneuver execution. The orbit solution and covariance is then mapped forward one week for designing the maneuver.

It is important that orbit errors don't grow substantially in this time frame. This covariance analysis included fitting the 10 days of data, then the orbit position and velocity uncertainties in the orbit-fixed frame (Radial, Along-track, Cross-track) were mapped into the future from 0 to 10 days ahead of the data cut-off to assess how the errors grow. Figure 3 illustrates how the $1-\sigma$ position uncertainties grow as a function of time from the DCO. The $1-\sigma$ velocity uncertainties are illustrated in Figure 4. From inspection of Figures 3 and 4 it becomes apparent that the orbital uncertainties remain fairly accurate in the seven day time frame. Position errors for this period remain below 100 m, while velocity uncertainties are less than 20 cm/s. As expected, Figure 3 shows that the along-track component dominates the position uncertainties. Less obvious is the fact that the radial component shown in Figure 4 dominates the velocity errors. After some consideration, it can be reasoned that this is directly related to the uncertainties in the physical parameters of Eros. Table 1 lists the $1-\sigma$ computed and considered position, and velocity uncertainties in the orbit-fixed frame after 7 days past the DCO. Also listed in Table 1 are the considered error contributions of the 8th degree and order gravity and the station location uncertainties.

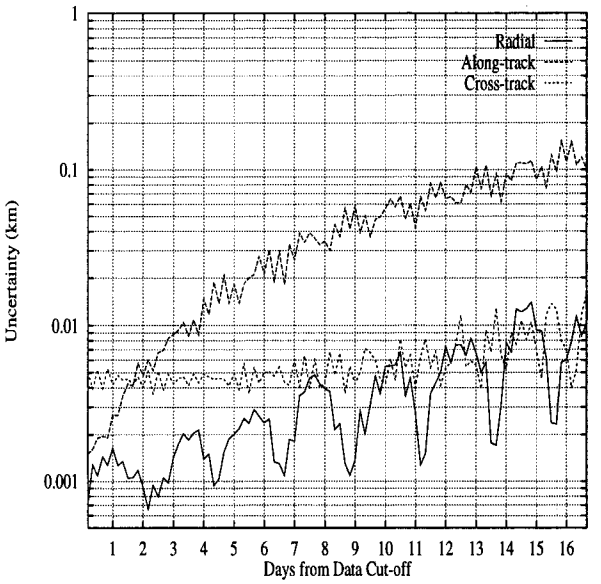

Figure 3: Orbit-fixed position (Radial, Along-track, Cross-track) $1-\sigma$ uncertainties as a function of time from DCO for the tight 25 km retrograde orbit.

Another covariance study was performed to determine how quickly after an OCM execution can the orbit be re-determined. This is important for updating the S/C trajectory for science pointing or for quick maneuver design in the case of emergencies. In this case, the orbit uncertainties are in real-time (i.e. not mapped forward in time). Figures 5 and ?? show how soon the $1-\sigma$ position and velocity errors return to steady state after an OCM executes with a 5 mm/s spherical uncertainty. It is shown from these figures that the orbit can be re-determined in less than 6 hours.

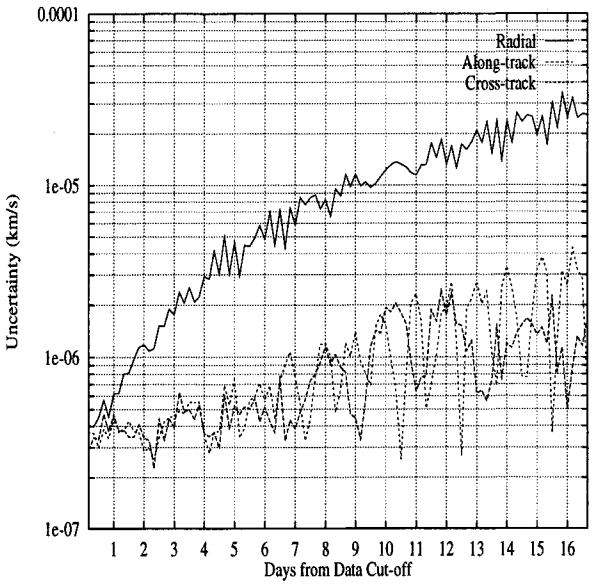

Figure 4: Orbit-fixed velocity (Radial, Along-track, Cross-track) $1-\sigma$ uncertainties as a function of time from DCO for the tight 25 km retrograde orbit

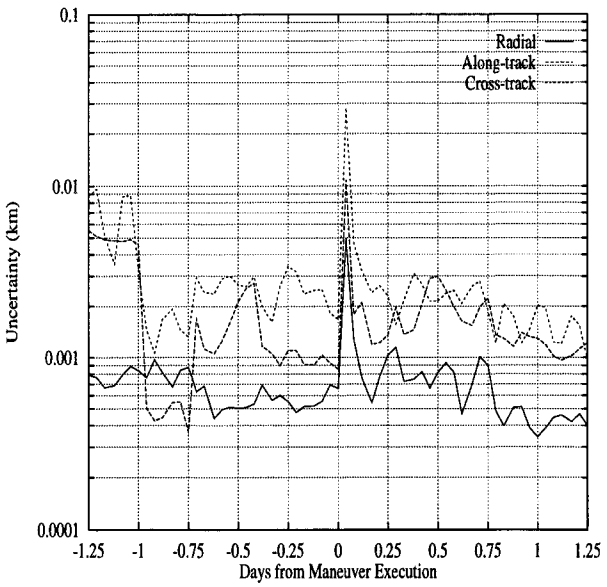

Figure 5: Orbit-fixed position (Radial, Along-track, Cross-track) $1-\sigma$ uncertainties as a function of time from maneuver execution for the tight 25 km retrograde orbit.

Low-Altitude Flyovers

Table 1: Position and velocity errors mapped to DCO+7 days

Run	Description	Position (m)		Velocity (mm/s)		
Error	Radial	Along-track	Cross-track	Radial	Along-track	Cross-track
Computed Covariance	0.75	11.22	1.59	2.49	0.19	0.23
Consider Covariance	1.82	26.11	6.07	5.83	0.38	0.77
Consider Contributions						
8th Degree and Order Gravity Harmonics	1.65	23.21	5.67	5.21	0.33	0.73
Station locations	0.14	4.08	1.48	0.86	0.04	0.04

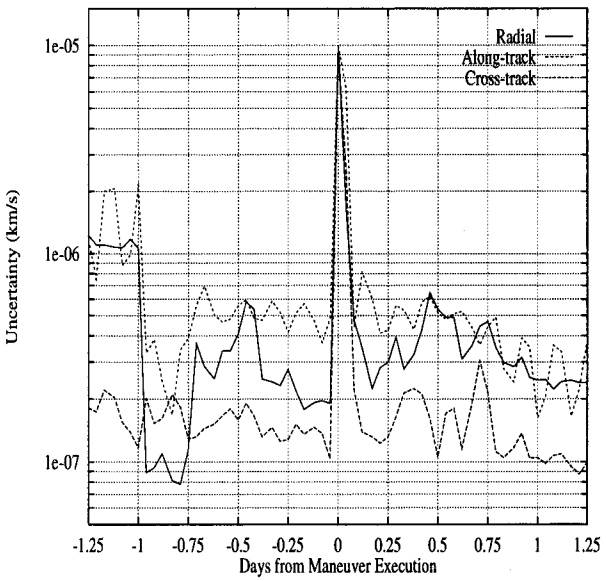

Figure 6: Orbit-fixed velocity (Radial, Along-track, Cross-track) $1-\sigma$ uncertainties as a function of time from maneuver execution for the tight 25 km retrograde orbit.

The analytical results detailed above also indicate another approach by which low altitude/high resolution images can be obtained from the asteroid surface. Knowing what the effects of a specific flyby of the asteroid will be, in terms of changes in the orbital elements, allows us to design the flybys to have "good" characteristic changes in orbit elements. If the S/C is initially in a circular orbit about the asteroid, a single properly timed maneuver can reduce and target the periapsis passage to a low altitude above a specific region of the asteroid. The flyby over this specific region will cause a change in the orbit elements, depending on the orbit inclination, node, and argument of periapsis (as measured in the body-fixed frame). There are three general cases that can occur: no major change in orbit energy, increase in orbit energy, decrease in orbit energy. These cases are simply controlled by the location of the periapsis in the body fixed frame, namely by the sign of $-\sin(2\tilde{\omega})$. A zero value of this term corresponds to no net change in energy, a negative value to a decrease in energy, a positive value to an increase in energy. The perturbations experienced can be quite major, as will be seen below, however a proper choice of flyby conditions can ensure that the S/C will not re-encounter the asteroid for an extended period of time.

A few specific flyby cases have been evaluated and are presented here. In all cases the apoapsis is at a radius of 50 km. Two cases are shown, with a periapsis at either 20 or 14 km. In both cases the transfer orbit period is approximately 12 hours. If the flyby decreases the energy, the semi-major axis decreases, the S/C apoapsis drops to a lower value and the S/C re-encounters the asteroid in a shorter time span, a situation that is not desirable from an operations or stability point of view. Conversely, if the flyby increases energy, the semi-major axis and period increase, leading to additional time in which to recircularize the orbit and prepare for the next encounter. In between these extremes, if the flyby is designed so as to leave the energy unchanged, the circularization maneuver must be performed at the next apoapsis, approximately 12 hours after the first maneuver.

In the following, we present plots and covariance analysis of the these three different types of low altitude passes. The specific trajectories are initially polar 50×14 km ellipses with periapsis in the equatorial plane and over the leading edge (at 45° longitude), over the trailing edge (at -45° longitude), and over the short side of the asteroid (at -90° longitude); and a 50×20 km ellipse with periapsis in the equator and over the long side of the asteroid (at 0° longitude). The radius variations are shown in Figure 7 and the semi-major axis and eccentricity variations are shown in Figures 8 and 9.

A covariance and monte-carlo analysis was performed for each of these flybys, assuming initial orbit uncertainties of 10 meters in position and 1 mm/sec in velocity ($1\text{-}\sigma$). The linear results agreed well with the monte-carlo results and are presented in Table 2. It is clear that none of these suffer major increases in uncertainty, and all will be close to the nominal trajectory following the flyby. Inspection of the Figures shows, however, that the trailing edge flyby is in the "safest" orbit following the low-altitude flyby as it is traveling to a much higher apoapsis radius (approximately 250 km for this case) en-

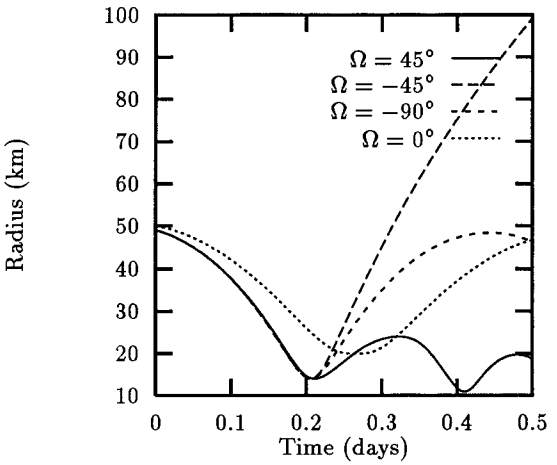

Figure 7: Radius variation of low-altitude flybys.

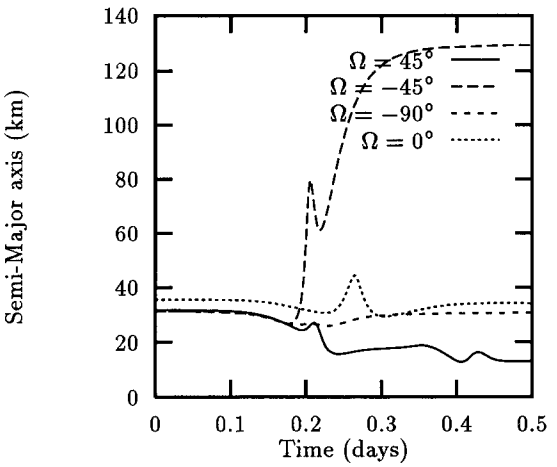

Figure 8: Semi-major axis variation of low-altitude flybys.

suring that there is sufficient time to re-establish control of the S/C prior to the next low-altitude pass. The leading edge flyby, however, has already traveled through a second periapsis passage before the end of the 12 hour period and is heading for its third passage, clearly an orbital situation to be avoided. The flybys of the short and long side of the asteroid do not yield significant change in the orbital elements but yield increased orbit determination uncertainties due to increased sensitivity to errors at these points.

LANDING TRAJECTORY DESIGN & NAVIGATION

At the end of the NEAR mission it is desired to place the S/C on the asteroid surface, obtaining additional scientific information in the process. Proposed here is a conservative approach to landing on the surface which should ensure that the S/C remain on the surface (i.e., does not become thrown from the surface following its impact), impact the surface with a minimal velocity, pro-

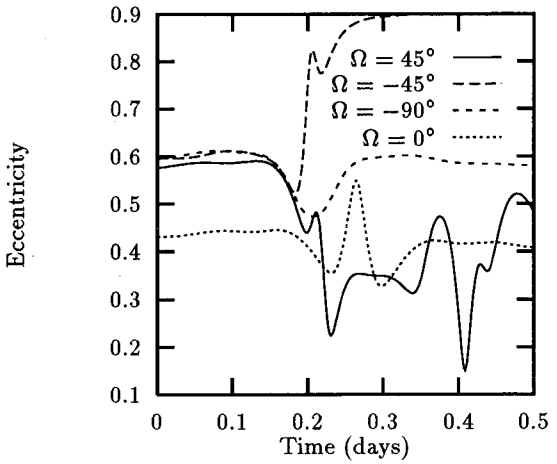

Figure 9: Eccentricity variation of low-altitude flybys.

Table 2: Predicted orbit uncertainties after one low-altitude flyby

Flyby Ellipse	Position 1-σ (km)	Velocity 1-σ (m/s)
14×50 $\Omega = -45°$	.15	.007
14×50 $\Omega = 45°$	.07	.019
14×50 $\Omega = -90°$	.24	.022
20×50 $\Omega = 0°$	.37	.371

vide an opportunity to obtain additional high-resolution images of the asteroid surface, and be executable without on-board autonomy beyond the current NEAR S/C capability. Also discussed are simple modifications to incorporate autonomous altitude measurements to enable lower landing speeds and enhance the capability of the S/C to acquire high-resolution surface images during this period. The basic scenario is simple: 1) place the S/C into a polar orbit about the asteroid; 2) when over the asteroid rotation pole perform a de-orbit maneuver to send the S/C onto an impact trajectory with the asteroid pole; 3) at a pre-determined time(s) perform slow-down maneuvers to retard the S/C fall rate; 4) perform an escape maneuver at a specified time to send the S/C away from Eros at a low escape speed during which ground contact is re-established; 5) after the orbit is re-determined and images taken during the sequence down-linked, repeat the procedure with the escape sequence designed to be less conservative (i.e., occur closer to the asteroid surface); 6) repeat the process until the S/C impacts with the asteroid surface. The landing itself would terminate one of these drop-in passes.

This process has several important features that will ease the operational aspects of its implementation. First, by targeting the landing to the asteroid pole, the issue of timing the S/C descent to be in phase with the asteroid rotational phase is removed, easing the design of

the landing trajectory and loosening up some of the uncertainty constraints. This also minimizes the surface relative speed of the S/C as the inertial velocity of the asteroid surface at the poles is near zero. Second, by making the initial "drop-ins" terminate early (i.e., by performing the escape maneuver conservatively early), the S/C is able to take additional images of the asteroid surface during the drop-in and relay them back to the Earth during the orbit re-acquisition period. Depending on the amount of time available to perform the entire landing sequence, the drop-in trajectory can be repeated several times, each time lowering the altitude of the escape sequence initiation. The S/C will eventually impact the surface, after which it is assumed that all systems will become inoperative and communications will cease.

This scenario has been simulated in a covariance study to estimate the likely uncertainties in footprint and altitude prior to a hypothetical impact on the asteroid surface ([7]). The orbit starts in a 30X30 km polar orbit. At the pole crossing a 9 m/s maneuver is performed to send the S/C down towards the pole with an initial velocity of 7 m/s. After 36 minutes the S/C is traveling downwards at 12 m/s where a final maneuver of 4.5 m/s is performed at an altitude of 3 km, setting up an impact of 10 m/s on the pole (at a radius of 7 km) within 6 minutes.

This trajectory has been analyzed assuming maneuver execution errors of 0.1 % in magnitude and 3 mrad in pointing. The error sources considered in the run are the a priori orbit determination uncertainty, the Eros mass uncertainty, the Eros 2nd degree and order gravity field uncertainty and the rotation rate uncertainty (it is assumed that Eros is in principal axis rotation). The errors are measured in the local coordinate frame fixed to Eros and centered at the impact site with local normal being defined as the z axis. A tight a priori OD uncertainty of 10 meters in position and 1 mm/sec in velocity is assumed 6 hours prior to the first maneuver. Table 3 spells out the computed and the consider covariance of this delivery.

For this analysis a larger value of $\mu \sim 1 \times 10 - 3$ km^3/s^2 is used, with a rotation period is 5.27 hours and nominal values of C_{20} = 35.1 km^2 and C_{22} = 17.55 km^2. As the landing will occur at the end of the mission, all of these parameters should be well established. In fact, the values used here are conservatively large, in general.

The issue of impact speed can be addressed, at first order, by a simple analysis of the trajectory. Assuming that a maneuver occurs at an altitude h above the surface of the asteroid pole, the impact speed will be (from the energy equation):

$$V_{\text{impact}} = \sqrt{\frac{2\mu h}{R(R+h)}} \qquad (20)$$

where R is the polar radius of the asteroid and μ is its GM value. Figure 10 shows a plot of this relation for different values of asteroid density. The above analysis indicates a 3-σ uncertainty in altitude of approximately 1.2 km. Thus, to ensure a given impact speed or an escape, the final maneuver must be performed before this altitude is reached, leading to an impact speed of 3 – 6 m/s, depending on the actual mass of 433 Eros.

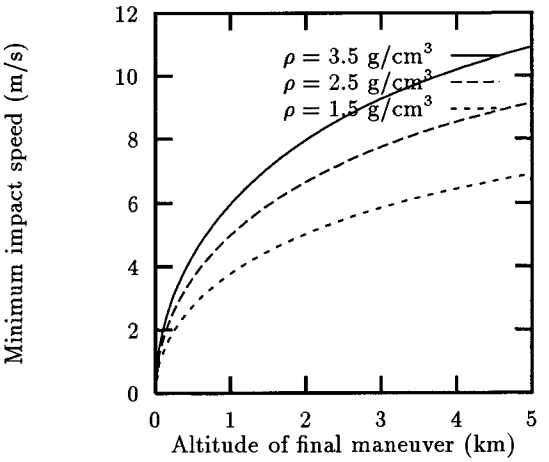

Figure 10: Minimum impact speeds as a function of final maneuver altitude, derived from the 2-body energy integral

The navigation challenge is to be able to execute the final maneuver as late as possible, as this will minimize the impact speed. The measurements available to the S/C during this time are its a priori solution prior to the de-orbit maneuver, the ACS which maintains the S/C attitude during the entire trajectory, and the accelerometers which are used to control the pre-planned maneuvers. To push the impact speed to an appreciably lower value, such as under 1 m/s, requires the inclusion of altimetry data into the navigation design, at least. There are three distinct levels of autonomy that can be incorporated here, increasing from simple to complex, that are spelled out below. We note that the footprint and lateral velocity uncertainties are small enough so that it is not crucial that they be sensed and corrected.

Autonomous Landing Design

The initial, and simplest, approach would have the S/C make altimetry measurements using the lidar after the initial descent has commenced. Due to its design the lidar cannot operate within a few (~5 km) of the asteroid surface. Thus these measurements must be taken shortly after the descent to the surface has commenced. If we assume that the S/C is following the nominal descent velocity profile, and its major errors are in absolute altitude above the surface, then a simple implementation is possible. The S/C would take a number of altitude measurements and compare them to the nominal descent profile and use the offset between them to shift the execution time of all subsequent maneuvers. This would allow for the position errors to be corrected for in the descent profile and would decrease the altitude uncertainty, but

Run Description	Cross-range (meters)	Vertical-range (meters)	Cross-speed (cm/sec)	Vertical-speed (cm/sec)
Computed Covariance	70	100	4	9
Consider Covariance	252	423	14	35
Consider Contributions				
Rotation uncertainty (0.001%)	183	301	10	25
Mass uncertainty (0.01%)	134	235	8	19
C_{20} and C_{22} uncertainty (>0.01%)	84	147	5	12

Table 3: Computed and Consider 1-σ covariance for the NEAR S/C landing on Eros

not the fall rate uncertainty. The implementation of this autonomous control would consist of comparing altitude measurements and their measurement epochs with the nominal profile and simply shifting the final time by the corresponding amount.

A slight modification of this scheme could yield substantially greater performance at the cost of S/W complexity. This would entail filtering the altitude measurements in time in order to estimate the fall rate of the S/C at some specified epoch (either in a current-time or batch sense). Modeling the landing dynamics as a one-dimensional problem, which is a feasible assumption here given the relatively good knowledge of the initial S/C state, allows new maneuver execution epochs to be estimated and updated. The proposed filter would be rather simple but would require a dedicated development period and budget to build, test and implement. Given the accuracy of the lidar measurement and the relatively short time between measurement and impact, the final maneuver altitude could be easily reduced to a few hundred meters or less.

If control over the landing footprint is desired, less than the 750 meter 3-σ result for the open loop control, it would be necessary to process optical data on-board the S/C during descent. This would entail a much more sophisticated algorithm, including routines to process images, correlate them with stored images to extract landmarks, and filter the measurements to extract relative position measurements with respect to the asteroid surface. This would be an interesting technology development but would be a capability that the NEAR S/C could not utilize fully as it cannot, in general, survive a surface landing. Given that the NEAR imager can write directly to the computer storage disk it is, however, an experiment that could be implemented.

The above discussions assume that the S/C is falling along the pole of the asteroid, so that the altimetry measurements are made relative to a surface whose radius is not changing in time. If these landing runs are desired to be made over other portions of the asteroid surface, the same basic methodology can be used again. The major change would be that the nominal profile of altitude measurements would have to be reduced against a more detailed model of the asteroid size as a function of the nominal S/C descent path. Again, a trajectory that falls radially would be the simplest to implement as the inertial latitude and longitude of the S/C would be fixed to within the control and knowledge ability of the ground-based operations. As the dynamic environment will be more severe in such a descent, the associated uncertainties in the footprint are expected to be relatively larger than those cited above.

CONCLUSIONS

Two feasible designs of low altitude passes have been considered in this study. These include the tight retrograde orbits that have the disadvantage of high relative speed with respect to the asteroid surface and low flybys of specific regions of the asteroid surface which have the advantage of lower relative speeds. The tight 25 km retrograde orbit shows promising accurate characteristics for navigation. It has been shown that the effects of OCM execution errors upon this orbit can be quickly ascertained. It should be cautioned, that in reality however, these accuracies may not always hold true. Furthermore, due to the highly dynamical environment that these orbits are subjected to, nonlinearities may cause orbit solution convergence problems. The orbit uncertainties for the low flyby passes have also been shown to remain within acceptable accuracies after periapses regardless of flying over the leading, or trailing edges or the ends of the asteroid. It has been shown that since the apoapsis is raised following a trailing edge flyby thereby ensuring sufficient time to re-establish orbit control, it maybe the safest to fly. A design for landing the spacecraft on the surface of Eros has been presented which includes successive drop-in passes, where the impacting speed is slowed down by maneuver execution at specified times then an escape maneuver is performed to re-establish orbit control and the process repeated to ensure the impacting speed is low enough that the S/C remains on the surface of Eros. It has been shown that the navigational accuracies allow for this design to be realized. For slower impact speeds, simple to complex strategies have been presented for autonomous landing by implementing the filtering of the LIDAR data or landmark tracking data on board the S/C.

ACKNOWLEDGEMENTS

The research described in this paper was carried out jointly by the Jet Propulsion Laboratory, California Institute of Technology, and the Johns Hopkins University,

Applied Physics Laboratory under contract with the National Aeronautics and Space Administration.

References

[1] D.K. Yeomans, "Asteroid 433 Eros: The Target Body of the NEAR Mission," *J. Astron. Sci.*, Vol. 43, No. 4, Oct-Dec 1995, pp 417-426.

[2] R.W. Farquhar, D.W. Dunham, J.V. McAdams, "NEAR Mission Overview and Trajectory Design," *J. Astron. Sci.*, Vol. 43, No. 4, Oct-Dec 1995, pp 353-371.

[3] J.K. Miller, B.G. Willliams, W.E. Bollman, R.P. Davis, C.E. Helfrich, D.J. Scheeres, S.P. Synnott, T.C. Wang, and D.K. Yeomans, "Navigation Analysis for Eros Rendezvous and Orbital Phases," *J. Astron. Sci.*, Vol. 43, No. 4, Oct-Dec 1995, pp 453-476.

[4] D.J. Scheeres, "Analysis of Orbital Motion Around 433 Eros", *J. Astron. Sci.*, Vol 43, No 4, Oct-Dec 1995, 427-452.

[5] J.K. Miller, E. Carranza, C.E. Helfrich, B.G. Williams, D.W. Dunham, R.W. Farquhar, Y. Gao, and J.V. McAdams,"Near Earth Asteroid Rendezvous (NEAR) Orbit Phase Trajectory Design," *AIAA/AAS Astrodynamics Conference*, Boston, MA, August 10-12, 1998, AIAA-98-4286.

[6] D.J. Scheeres, F. Marzari, L. Tomasella, V. Vanzani, "ROSETTA mission: satellite orbits around a cometary nucleus", Planetary and Space Science, *in press.*

[7] D.J. Scheeres, "Interactions between ground-based and autonomous navigation for precision landing at small solar-system bodies", *Telecommunications and Data Acquisition Progress Reports*, 42-132, February 15, 1998.

[8] D.J. Scheeres, S.J. Ostro, R.S. Hudson, R.A. Werner, "Orbits Close to Asteroid 4769 Castalia", *Icarus*, **121**, pp 67-87, 1996

[9] D.J. Scheeres, "Dynamics About Uniformly Rotating Tri-Axial Ellipsoids. Applications to Asteroids", *Icarus*, Vol 110, pp 225 - 238, 1994.